Molecular Therapy
Original Article

mRNA Therapy Improves Metabolic and Behavioral Abnormalities in a Murine Model of Citrin Deficiency

Jingsong Cao,[1] Ding An,[1] Mikel Galduroz,[1] Jenny Zhuo,[1] Shi Liang,[1] Marianne Eybye,[1] Andrea Frassetto,[1] Eishi Kuroda,[2] Aki Funahashi,[2] Jordan Santana,[1] Cosmin Mihai,[1] Kerry E. Benenato,[1] E. Sathyajith Kumarasinghe,[1] Staci Sabnis,[1] Timothy Salerno,[1] Kimberly Coughlan,[1] Edward J. Miracco,[1] Becca Levy,[1] Gilles Besin,[1] Joshua Schultz,[1] Christine Lukacs,[1] Lin Guey,[1] Patrick Finn,[1] Tatsuhiko Furukawa,[2] Paloma H. Giangrande,[1] Takeyori Saheki,[2] and Paolo G.V. Martini[1]

[1]Moderna, Inc., Cambridge, MA, USA; [2]Department of Molecular Oncology, Kagoshima University, Kagoshima, Japan

Citrin deficiency is an autosomal recessive disorder caused by loss-of-function mutations in *SLC25A13*, encoding the liver-specific mitochondrial aspartate/glutamate transporter. It has a broad spectrum of clinical phenotypes, including life-threatening neurological complications. Conventional protein replacement therapy is not an option for these patients because of drug delivery hurdles, and current gene therapy approaches (e.g., AAV) have been hampered by immunogenicity and genotoxicity. Although dietary approaches have shown some benefits in managing citrin deficiency, the only curative treatment option for these patients is liver transplantation, which is high-risk and associated with long-term complications because of chronic immunosuppression. To develop a new class of therapy for citrin deficiency, codon-optimized mRNA encoding human citrin (hCitrin) was encapsulated in lipid nanoparticles (LNPs). We demonstrate the efficacy of hCitrin-mRNA-LNP therapy in cultured human cells and in a murine model of citrin deficiency that resembles the human condition. Of note, intravenous (i.v.) administration of the hCitrin-mRNA resulted in a significant reduction in (1) hepatic citrulline and blood ammonia levels following oral sucrose challenge and (2) sucrose aversion, hallmarks of hCitrin deficiency. In conclusion, mRNA-LNP therapy could have a significant therapeutic effect on the treatment of citrin deficiency and other mitochondrial enzymopathies with limited treatment options.

INTRODUCTION

Type II citrullinemia (CTLN2) is an adult-onset autosomal recessive disease caused by mutations in *SLC25A13*, which encodes a liver-specific aspartate (Asp)/glutamate transporter called citrin that is localized in the inner membrane of mitochondria.[1–3] Citrin serves a critical function as a carrier of Asp from mitochondria to the cytosol, where it enters the urea cycle by condensing with citrulline to form argininosuccinate, a step catalyzed by argininosuccinate synthetase (ASS).[4] In humans, citrin deficiency causes accumulation of citrulline in the liver and plasma and subsequent failure of the urea cycle to efficiently clear ammonia from the blood stream, resulting in hyperammonemia.[1] It is believed that the accumulation of citrulline in CTLN2 patients is caused by two possible mechanisms: (1) unavailability of Asp as a substrate for ASS and (2) loss of ASS protein.[5,6]

Unlike the classic neonatal and infantile type I citrullinemia (CTLN1), which is caused by deficiency of the *ASS* gene, CTLN2 is clinically characterized by adult-onset features such as serious and recurring hyperammonemia and associated neurological symptoms, including disorientation, delusion, unconsciousness, seizures, hypersensitivity, and coma.[3,7] These neurological symptoms, often triggered by illness, medication, over-ingestion of carbohydrates, or alcohol consumption in a subset of CTLN2 patients, persist for prolonged periods of time and can lead to irreversible encephalopathy and death. The discovery of *SLC25A13* as the disease-causing gene and further identification of its function as a mitochondrial Asp/glutamate transporter have greatly advanced our understanding of CTLN2 and improved diagnosis and management of the disease.[1–3] In addition to the adult-onset form, referred to as CTLN2, *SLC25A13* mutations in patients can also result in two additional disease phenotypes: neonatal intrahepatic cholestasis (NICCD) and failure to thrive and dyslipidemia (FTTDCD).[8–10] All three disorders, which stem from citrin deficiency, are typically managed with diet (e.g., low carbohydrate and high protein and fat) and supplements (e.g., administration of arginine and/or sodium pyruvate).[11–14] However, these interventions are limited because of patient compliance, limited efficacy, and undesired side effects.[13] Liver transplantation remains the only curative option for this disease.

Protein replacement therapy (like enzyme replacement therapy [ERT]) has proven successful in treating inherited metabolic diseases

Received 4 October 2018; accepted 19 April 2019;
https://doi.org/10.1016/j.ymthe.2019.04.017.

Correspondence: Paolo G.V. Martini, Moderna, Inc., 500 Technology Square, 7th Floor, Cambridge, MA 02139, USA.
E-mail: paolo.martini@modernatx.com

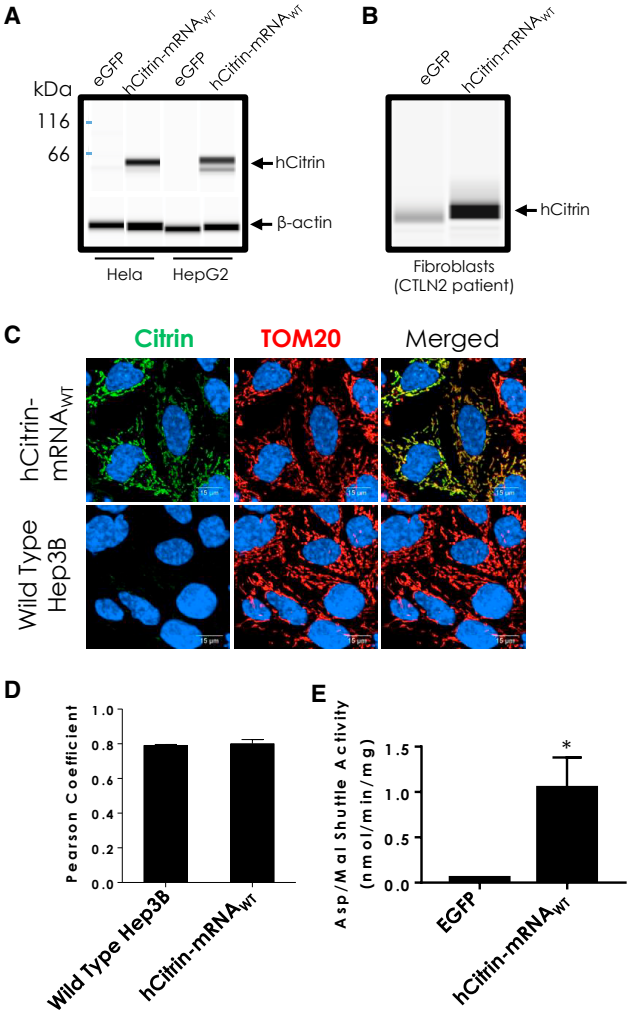

Figure 1. Citrin Protein Expression Levels in Mammalian Cell Lines Transfected with hCitrin-mRNA

(A and B) Modified mRNAs consisting of the open reading frame of the wild-type hCitrin nucleotide sequence (hCitrin-mRNA$_{WT}$) or EGFP (1 μg) were transfected into (A) HeLa and HepG2 cells or (B) CTLN2 patient fibroblasts. Twenty-four hours post-transfection, cell lysates were processed by capillary electrophoresis (CE) to assess protein expression levels. (C) Immunocytochemistry of exogenously expressed hCitrin in Hep3B cells. Cells were transfected with hCitrin-mRNA$_{WT}$ and analyzed with confocal microscopy for co-localization with the mitochondrial marker TOM20. Non-transfected cells (wild-type Hep3B) showed very low levels of endogenous Citrin, whereas cells transfected with the hCitrin-mRNA$_{WT}$ showed significantly higher protein levels, which colocalized with TOM20. The cells were also counterstained with DAPI (blue) for nucleus visualization. (D) Image analysis showed similar co-localization with mitochondrial markers for untransfected and hCitrin-mRNA$_{WT}$-transfected cells (Pearson coefficient values of 0.79, and 0.8, respectively). (E) Malate/aspartate transporting activity in isolated mitochondria prepared from HepG2 cells transfected with EGFP or hCitrin-mRNA. Data are represented as mean ± SEM (n = 3, independent experiments). Student's t test (*p < 0.05 versus EGFP) was performed to assess statistically relevant differences between groups.

such as lysosomal storage diseases.[15] However, this strategy has several limitations for therapeutic applications involving intracellular membrane-associated proteins. Viral vectors have recently shown promise for gene replacement therapy of intracellular proteins. Despite advances in viral vector delivery technology, inherent risks remain in terms of insertional mutagenesis (e.g., genotoxicity) and immunogenicity.[16] To overcome many of these concerns, we examine the use of mRNA therapy delivered via lipid nanoparticles (LNPs) for a variety of human diseases, including infectious diseases, cancer, and inherited metabolic liver diseases.[17,18] Delivery of mRNA for therapeutic use offers many advantages over traditional ERT or gene therapy: (1) it utilizes the endogenous intracellular translational and trafficking machinery to express functional intracellular and membrane-bound proteins; (2) it does not cause permanent changes to the genome, avoiding insertional mutagenesis risks; and (3) dosing regimens can be readily controlled based on medical conditions and patients' needs.

In this study, we investigated a novel mRNA-based therapy for the treatment of citrin deficiency. We produced and screened a series of chemically modified and codon-optimized mRNA variants encoding human citrin (hCitrin) and examined the effectiveness of select hCitrin-mRNAs in a clinically relevant citrin-deficient mouse model.

RESULTS

Characterization of hCitrin-mRNA$_{WT}$ Expression Levels, Subcellular Localization, and Activity in Mammalian Cells in Culture

We have developed a platform technology for generating immune-silent mRNAs that can treat a number of diseases, including inherited metabolic disorders.[17–22] As a proof of concept, we synthesized an mRNA that used the coding sequence from wild-type hCitrin (hCitrin-mRNA$_{WT}$). To test whether this construct resulted in full-length hCitrin protein, we first analyzed protein expression in cultured mammalian cells transiently transfected with hCitrin-mRNA$_{WT}$ (Figure 1A). As shown in Figure 1A, hCitrin-mRNA$_{WT}$ transfected in either HeLa or HepG2 cells resulted in robust expression of hCitrin protein at the expected molecular weight (~66 kDa). Robust hCitrin protein expression was also confirmed in CTLN2 patient fibroblasts transiently transfected with hCitrin-mRNA$_{WT}$ (Figure 1B). To determine whether the exogenous hCitrin protein was properly localized to the mitochondria, we performed immunocytochemistry for hCitrin and TOM20 (mitochondrial import receptor subunit TOM20, a mitochondrial marker protein)[23] in a human liver cell line (Hep3B) transfected with hCitrin-mRNA$_{WT}$. Our confocal microscopy analysis demonstrated strong colocalization between hCitrin and TOM20, confirming proper subcellular localization of the exogenous hCitrin to mitochondria (Figure 1C). Computational image analysis using an algorithm to calculate the Pearson's colocalization coefficient also demonstrated robust and significant colocalization between the staining of hCitrin and TOM20 (Figure 1D).

To determine whether hCitrin-mRNA$_{WT}$ encodes a functional protein, we measured citrin transport activity using the malate

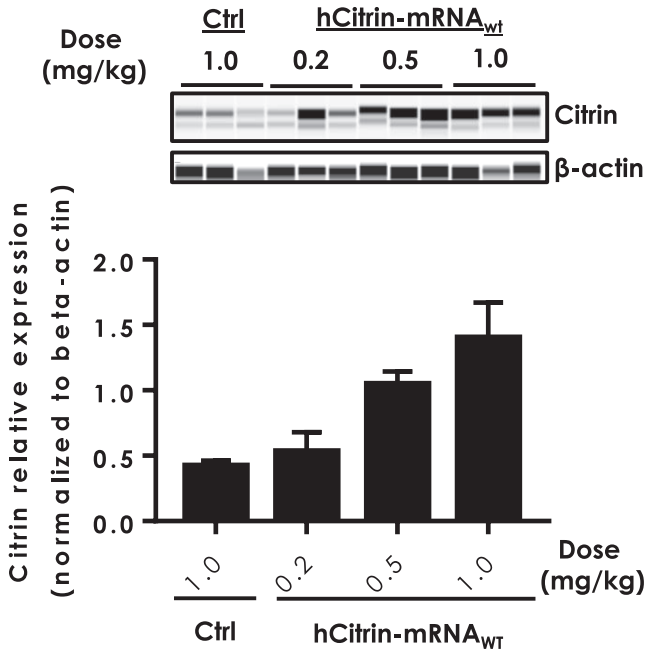

Figure 2. Citrin Protein Expression Levels in Livers of Wild-Type Mice Treated with hCitrin-mRNA Encapsulated in LNP

C57BL/6 mice were injected (i.v.) with LNP containing either a non-specific control mRNA (Ctrl) or hCitrin-mRNA. Mice were euthanized 24 h post-injection and evaluated for hCitrin protein levels in liver homogenates using CE (top). hCitrin protein expression levels were quantified, normalized to β-actin, and represented as mean ± SEM (bottom, n = 3).

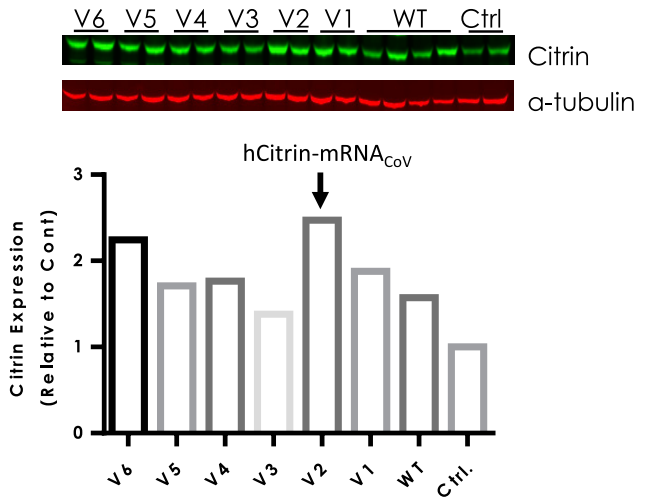

Figure 3. Citrin Protein Expression Levels in Wild-Type Mice Administered hCitrin-mRNA Variants Encapsulated in LNP

C57BL/6 mice were injected (i.v.) with either a non-specific control mRNA (Ctrl), hCitrin-mRNA$_{WT}$ (WT), or codon-optimized mRNA variants encoding hCitrin (V1–V6). Mice were euthanized 24 h post-injection, and hCitrin protein expression levels were detected by immunoblot analysis from liver tissue homogenates and normalized to α-tubulin. Citrin and α-tubulin protein expression levels were quantified using the Odyssey CLx instrument and accompanying software. Citrin-to-α-tubulin ratios were graphed as mean values (n = 2).

(Mal)/Asp shuttle assay in mitochondrial preparations from HepG2 cells transfected with either a control (Ctrl) mRNA (encoding EGFP) or hCitrin-mRNA$_{WT}$. In contrast to mitochondrial extracts from EGFP-expressing cells, mitochondrial preparations from hCitrin-mRNA$_{WT}$ expressing HepG2 cells exhibited a robust increase in Mal/Asp shuttle activity (Figure 1E), confirming a functional hCitrin protein being introduced by the hCitrin-mRNA.

Characterization of hCitrin-mRNA Therapy *In Vivo*

The use of lipid nanoparticles (LNPs) to deliver mRNA has been extensively studied[24,25]. To this end, we have developed proprietary lipids that have demonstrated both safe and effective delivery of therapeutic mRNAs to the liver in mouse models. We have coupled these novel lipids with advances in mRNA chemistry and design to enable both the safe and effective delivery of mRNA *in vivo*.[19,22] To assess whether this system delivers hCitrin-mRNA$_{WT}$ *in vivo* to mouse livers, we injected normal C57BL/6 mice intravenously (i.v.) with LNP containing either a non-translating control mRNA (Ctrl) or hCitrin-mRNA$_{WT}$ and measured the hepatic expression of hCitrin protein. Mice were sacrificed at 24 h post-injection, and hCitrin protein levels in liver mitochondrial preparations were determined by a capillary electrophoresis (CE)-based western system. As shown in Figure 2, i.v. injection of LNP-formulated hCitrin-mRNA$_{WT}$ yielded a dose-dependent increase in hCitrin protein in mouse liver, demonstrating that hCitrin-mRNA$_{WT}$ expresses hCitrin *in vivo*.

In recent years, codon optimization has been widely used to enhance protein expression for various mRNA-based therapeutic applications.[26] To investigate the effect of codon choice on hCitrin expression, we produced six independent codon-optimized hCitrin-mRNAs (V1–V6). This led to identification of a citrin-mRNA variant (hCitrin-mRNA$_{CoV}$) with a more than 50% increase in hCitrin expression in mouse liver compared with hCitrin-mRNA$_{WT}$ (Figure 3). Note that the primary antibody (Ab) used in Figures 2 and 3 was NBP1-89019 (Novus Biologicals), which has a preference in recognizing human versus murine citrin (with a higher sensitivity for detecting hCitrin, data not shown).

Efficacy of hCitrin-mRNA Therapy in CTLN2 Mice

We next examined the hepatic expression of hCitrin protein in *Slc25a13*-knockout (KO) (also known as citrin knockout [*Ctrn*-KO]) mice after systemic delivery of hCitrin-mRNA$_{CoV}$. We identified an Ab (TA-332958 from OriGene) that has good cross-reactivity against both human and mouse citrin. Similar levels of hCitrin and mouse citrin (mCitrin) proteins were detected by TA-332958 in HeLa cells transfected with equal amounts of hCitrin or mCitrin-mRNA (data not shown). As measured by immunoblot analysis using this Ab, i.v. injection of hCitrin-mRNA$_{CoV}$ at 0.5 mg/kg in *Ctrn*-KO mice led to expression of hCitrin protein compared with *Ctrn*-KO mice treated with a Ctrl mRNA (Figure 4). Although western blotting is not the most sensitive and quantitative technique for protein quantification, our analysis showed a wide range of linearity, covering the signals of citrin bands from both original and serially diluted

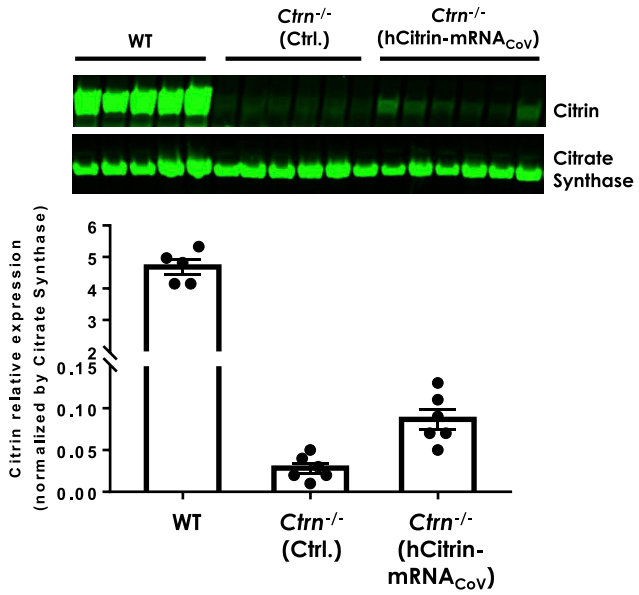

Figure 4. Citrin Protein Expression Levels in Citrin-Deficient Mice

Ctrn$^{-/-}$ mice were injected (i.v.) with either Ctrl or hCitrin-mRNA at 0.5 mg/kg. Mice were euthanized 24 h post-injection. Citrin protein expression levels in mitochondria prepared from mouse livers were assessed by immunoblot analysis and normalized to citrate synthase (CS), a mitochondrial marker. Citrin and CS protein expression levels were quantified using the Odyssey CLx instrument and accompanying software. Bars represent mean ± SEM (n = 5–6).

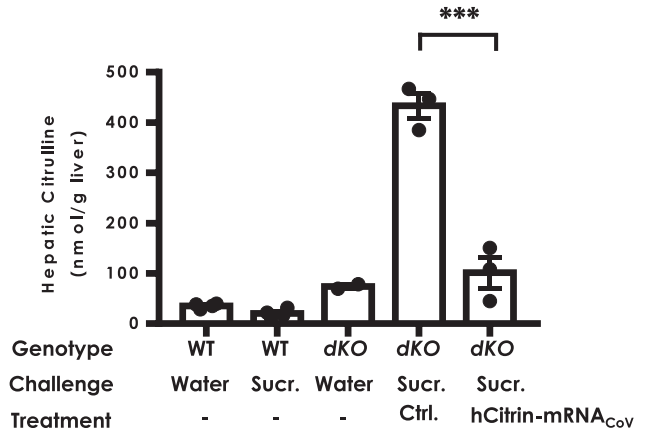

Figure 5. Effect of hCitrin-mRNA Therapy on Hepatic Citrulline Levels in the CTLN2 Mouse Model following Sucrose Challenge

Mice with different genetic backgrounds were first injected (i.v.) with LNP containing either EGFP (Ctrl) or hCitrin-mRNAs (hCitrin-mRNA$_{CoV}$) (0.5 mg/kg). 24 h post-injection, the mice were challenged by oral administration of the indicated test solution: pure water (Water) or 50% sucrose solution (Sucr.) at 20 mL/kg body weight. One hour following the sucrose challenge, the mice were euthanized, and livers were collected for citrulline analysis by LC-MS. WT, wild-type mice; dKO, mice with deletion for both mitochondrial glycerol-3 phosphate dehydrogenase (mG3PD) and citrin. The data are represented as mean ± SEM (n = 3–4 per group). One-way ANOVA and Dunnett's t test were performed to determine a statistically relevant difference between the groups. ***$p < 0.001$.

wild-type (WT) mitochondrial preparations (Figure S1A). We estimate that ~2%–5% of endogenous mCitrin levels in WT mice were restored in hCitrin-mRNA$_{CoV}$-treated *Ctrn*-KO mice 24 h post-injection (Figure 4; Figure S1B).

Having demonstrated the mitochondrion-targeted expression of a functional hCitrin protein *in vitro* and enhanced hepatic protein expression *in vivo* by hCitrin-mRNA$_{CoV}$, we next investigated the *in vivo* efficacy of the LNP-formulated hCitrin-mRNA$_{CoV}$ in mouse models of CTLN2. The KO mouse model with a single deletion of *Slc25a13* or citrin (*Ctrn*-KO) has been well characterized.[27] Although *Ctrn*-KO mice exhibited biochemical deficiency of both *in vitro* Mal/Asp transporting activity in liver mitochondrial preparations and *ex vivo* gluconeogenesis and ureagenesis in the perfused liver model, they failed to show any significant physiological abnormalities *in vivo*, such as citrullemia and hyperammonia, the hallmarks of human CTLN2. To establish a more representative CTLN2 mouse model, Saheki et al.[27] generated a mouse line with a double deletion of *citrin* and *mGPD* (encoding the mitochondrial glycerol 3-phosphate dehydrogenase; *Ctrn/mGPD*-double KO [dKO]). Like human CTLN2, *Ctrn/mGPD*-dKO mice had a dramatic elevation in hepatic citrulline levels upon challenge with some precipitating factors such as ethanol and sucrose.[28] Therefore, we used hepatic citrulline as a biomarker in the *Ctrn/mGPD*-dKO model to evaluate the pharmacological effects of hCitrin-mRNA$_{CoV}$. Consistent with previous reports[28], oral administration of 50% sucrose elicited dramatic elevation in hepatic citrulline in *Ctrn/mGPD*-dKO mice (Figure 5). A single i.v. administration of hCitrin-mRNA$_{CoV}$ at 0.5 mg/kg 1 day before the sucrose challenges caused a significant reduction in hepatic citrulline compared with mice treated with a Ctrl mRNA (Figure 5).

Another hallmark of clinical presentation in CTLN2 patients is a strong preference for lipid- or protein-enriched food and avoidance of food high in carbohydrates.[29] This clinical feature was also recapitulated in *Ctrn/mGPD*-dKO mice, which showed significant aversion to sucrose solution compared with single *Ctrn*-KO, *mGPD*-KO, or WT mice.[28] In view of its close resemblance to CTLN2 and noninvasiveness, we used this model to assess the efficacy of hCitrin-mRNA$_{CoV}$. In this study, single-housed *Ctrn/mGPD*-dKO mice received three 0.5 mg/kg weekly i.v. injections of either a Ctrl mRNA (Ctrl) or hCitrin-mRNA$_{CoV}$ (hCitrin). The effect of the mRNAs on voluntary sucrose intake was measured over the course of 48 h, as reported previously.[28] Specifically, voluntary sucrose intake was assessed before and after administration of the second dose of mRNAs. As shown in Figure 6A, left, no significant difference in voluntary sucrose intake between Ctrl and hCitrin-mRNA$_{CoV}$ groups was observed before treatment. In contrast, treatment with the hCitrin-mRNA$_{CoV}$ resulted in a significant increase in sucrose consumption in *Ctrn/mGPD*-dKO mice in comparison with mice treated with a Ctrl mRNA (Figure 6A, right). As reported previously, WT mice and mice with single deletion of *mGPD* or *citrin* exhibited an almost 100% preference for the sucrose solution[28].

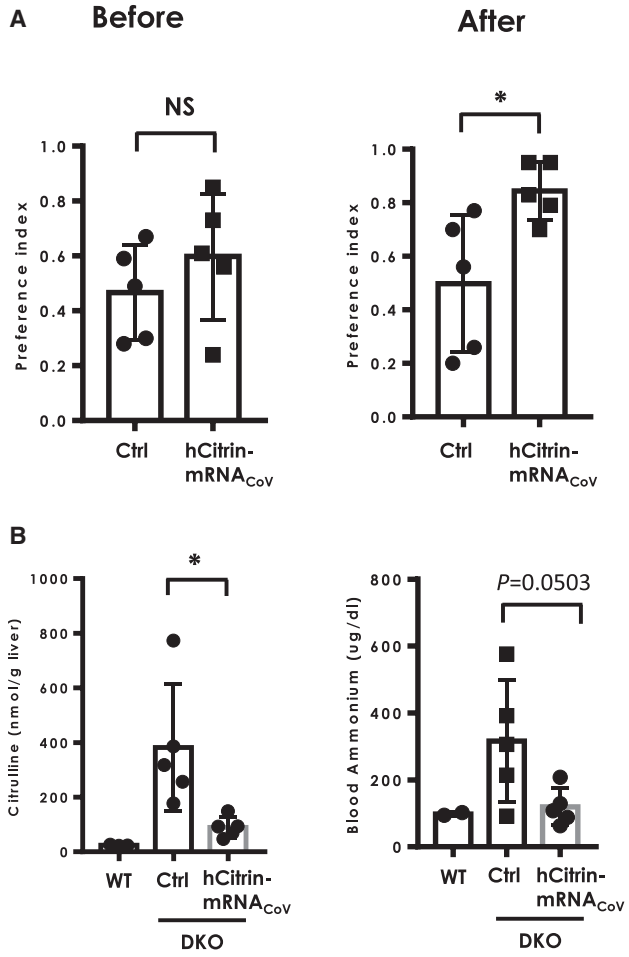

Figure 6. Effect of hCitrin-mRNA Therapy on Sucrose Aversion and Blood Ammonia in the CTLN2 Mouse Model

(A) Effect of hCitrin-mRNA therapy on sucrose aversion in CTLN2 mice. Preference index: intake of 20% sucrose versus water that was measured before (left) or after (right) mRNA therapy. (B) Effect of hCitrin-mRNA therapy on hepatic citrulline (left) and blood ammonia (right) in CTLN2 mice following sucrose challenge. CTLN2 mice were injected intravenously (i.v.) with LNPs containing either a non-specific control mRNA (Ctrl) or the hCitrin-mRNA$_{CoV}$ (0.5 mg/kg). Twenty-four hours following mRNA injection, the mice were challenged by oral administration of 50% sucrose, followed by collection of the liver for citrulline analysis and plasma for ammonium analysis (Materials and Methods). The data are expressed as mean ± SEM (n = 3–5 per group). Student's t test was performed to assess statistical relevance between the groups. *p < 0.05; NS, not significant.

As reported previously,[30] *Ctrn/mGPD*-dKO mice also exhibited hyperammonemia after an oral sucrose challenge, a feature that was also observed in CTLN2 patients.[31] To determine whether hCitrin-mRNA$_{CoV}$ treatment had any effect on plasma ammonia in this model, the same cohort of *Ctrn/mGPD-dKO* mice used in the sucrose aversion test was challenged with a solution containing 50% sucrose 24 h after the third and final dose. Hepatic citrulline and blood ammonia levels were performed 1 h after challenge. As shown in Figure 6B, left panel, administration of hCitrin-mRNA$_{CoV}$ resulted in a significant reduction in hepatic citrulline in this study. Consistent with the improved hepatic citrulline level, blood ammonia in mice treated with hCitrin-mRNA$_{CoV}$ showed a trend toward a significant decrease compared with the Ctrl mRNA-treated group (Figure 6B, right, p = 0.0503). Levels of hCitrin protein after administration of three doses of hCitrin-mRNA$_{CoV}$ were consistent with results from a single dose (i.e., ~2%–5% of the WT level; Figure S1). During this study, we did not observe treatment-related severe adverse effects or animal deaths, and there was no significant difference in body weight among different treatment groups (data not shown).

DISCUSSION

The discovery of bi-allelic pathogenic mutations of *SLC25A13* (encoding citrin, an Asp/glutamate transporter) as the genetic cause of the adult-onset CTLN2 and other neonatal or early-onset forms of citrin-deficient diseases (i.e, NICCD and FTTDCD) have greatly advanced our understanding of the molecular pathogenesis and the clinical diagnosis and management of these diseases.[1–3,32–34] However, citrin deficiency, especially CTLN2, remains a urea cycle disorder with a relatively poor prognosis. This is mainly due to recurring episodes of severe hyperammonemic crises and associated encephalopathy in a subset of affected patients. These episodes are often accompanied by other advanced liver diseases such as cirrhosis and liver failure and lack of targeted therapies for fast-onset and effective relief. Despite the significant improvement seen with restrictive dietary interventions, many patients still suffer irreversible brain damage and even death.[13] In addition, these dietary interventions have side effects and other undesired long-term complications. To our knowledge, no gene therapy or other disease-modifying agents have been developed for the treatment of hCitrin deficiency, and liver transplantation remains the only curative option for affected patients.

We are focused on developing mRNA-based therapies as a novel strategy for the treatment of otherwise intractable inherited errors in metabolism (IEMs). Because the primary sequence of a given protein carries all information that is needed for its proper subcellular localization (i.e., intracellular or membrane) and function, introducing mRNA into cells to direct protein biosynthesis with their own translational machineries is poised to enable the expression of a functional protein to correct related inherited diseases that are otherwise intractable with traditional approaches. Delivery of mRNA to cells by LNP bypasses insertional mutagenesis, carcinogenesis, and immunogenicity risks associated with traditional gene therapies delivered via viral vectors. Recently, we have demonstrated robust hepatic expression of the intracellular proteins (e.g., mitochondrial methylmalonyl-coenzyme A [CoA] mutase and cytoplasmic porphobilinogen deaminase) with chemically modified, codon sequence-optimized mRNAs encapsulated in LNPs. Of note, these lipid-mRNA formulations have resulted in safe and effective correction of metabolic abnormalities in mouse models of disease.[17,21] In the present study, we sought to develop an mRNA-based therapy targeting CTLN2 and citrin, the affected transporter protein that is also localized in the mitochondrial matrix.

We first demonstrated that hCitrin-mRNA, when transfected into mammalian cells, led to translation of a functional citrin protein localized to mitochondria and conferred a robust mitochondrial Mal/Asp transporting activity in a liver cell line, HepG2 (Figure 1). We next assessed *in vivo* expression and efficacy in murine models of CTLN2. LNP-encapsulated mRNAs have been successfully delivered *in vivo* in both preclinical and clinical settings.[35–39] We used our proprietary LNP formulation system to deliver hCitrin-mRNA into hepatocytes *in vivo* and achieved dose-dependent expression of hCitrin protein in murine livers (Figure 2). Encouraged by these results, we next screened a series of codon-optimized hCitrin-mRNAs by examining their hepatic protein expression in cellular and murine models. Through several rounds of screening, a codon-optimized hCitrin-mRNA variant (hCitrin-mRNA$_{CoV}$) was identified and tested further in CTLN2 mouse models.

The *Ctrn* KO (*Ctrn*$^{-/-}$) mouse model has been well characterized,[27] and although *Ctrn*$^{-/-}$ mice exhibited significant deficiency in Asp/Mal shuttling activity and other pathways where Citrin is critically involved, they failed to show CTLN2-like symptoms (*i.e.*, hyperammonemia and perturbation in amino acid metabolism). It has been postulated that the lack of pathological phenotypes of *Ctrn*$^{-/-}$ mice is due to very high levels of glycerol-3 phosphate shuttling activity in the liver, which could compensate for the loss of citrin-driving nicotinamide adenine dinucleotide-hydrogen (reduced) (NADH) shuttling. Based on this hypothesis, Saheki et al.[30] established a mouse model with deletion of both citrin and mitochondrial glycerol 3-phosphate dehydrogenase (mGPDH) (*Ctrn/mGPD*-dKO), which indeed showed many of the same features of human CTLN2, including citrullinemia and hyperammonemia, which were further exacerbated by oral sucrose administration. Furthermore, *Ctrn/mGPD*-dKO mice also showed a dramatic surge in hepatic citrulline upon oral ethanol or sucrose challenge, a prominent feature directly caused by citrin deficiency and associated with disease manifestation in human CTLN2. Therefore, we used the *Ctrn/mGPD*-dKO mouse model to assess the efficacy of our lead hCitrin-mRNA construct in lowering hepatic citrulline upon sucrose challenge. hCitrin-mRNA$_{CoV}$ resulted in a significant reduction in hepatic citrulline in *Ctrn/mGPD*-dKO mice challenged with sucrose, suggesting effectiveness of hCitrin-mRNA$_{CoV}$ in this disease model. Very recently, Saheki et al.[28] described an oral aversion model in which *Ctrn/mGPD*-dKO mice showed a strong decrease in voluntary oral intake of sucrose solution in comparison with WT mice or mice with single deletion of either *citrin* or *mGPD*. This feature mirrors the clinical presentation of human CTLN2 well because these patients also show a strong preference for protein- or lipid-enriched food versus carbohydrate-enriched food, and intake of a high level of sucrose or fructose is among precipitating factors in the development of citrullinemia and hyperammonemia. Therefore, we used the sucrose aversion test to examine the pharmacological efficacy of hCitrin-mRNA$_{CoV}$. Administration of hCitrin-mRNA$_{CoV}$ led to less aversion of sucrose solution intake, along with a decrease in hepatic citrulline level and a trend toward decreased blood ammonia, demonstrating the effectiveness of our mRNA construct in correcting the behavioral abnormalities caused by citrin deficiency (Figure 6).

Metabolic and behavioral perturbation caused by citrin deficiency was rescued by exogenously administered hCitrin protein at ~2%–5% of the WT (based on endogenous mCitrin protein levels) (Figure 4; Figure S1; Figure 6). Clinically, citrin deficiency is a very heterogeneous disorder.[40] Although a clear genotype-phenotype correlation remains elusive, it is hypothesized that CLTN2 is caused by a complete deficiency of citrin, and many patients may remain asymptomatic during their lifetimes.[41] It is also worth noting that the majority (>90%) of disease-causing citrin mutations result in the absence of citrin protein, likely because of rapid protein degradation of the truncated or mislocalized proteins.[1,41–44] Thus, partial restoration of citrin protein levels is expected to result in a significant clinical outcome.

Despite recent advances in understanding the molecular genetics and pathogenesis of CTLN2, treatment options remain limited. This is especially true for a subset of patients with sudden onset of severe hyperammonemia and encephalopathy who may present with additional liver problems, including cirrhosis, liver failure, and hepatocellular carcinoma, and require immediate treatment to avoid irreversible brain damage and death. The mRNA-based therapies described here are expected to provide such a treatment option over the current standard of care (i.e., dietary intervention or glycerol phenylbutyrate to control blood ammonia levels) for such a subset of affected patients, either as a one-time emergency treatment or long-term maintenance therapy.

In summary, we have demonstrated for the first time that an mRNA-based therapy could be effective in an animal model of CTLN2 and provided a preclinical proof of concept for targeting citrin-deficient human diseases. Our data also warrant further investigation and optimization to improve the efficacy and safety of hCitrin-mRNA-based therapeutics.

MATERIALS AND METHODS

mRNAs and LNP Formulations

Complete N1-methylpseudouridine- or 5-methoxyuridine-substituted mRNA was synthesized *in vitro* from a linearized DNA template containing the 5′ and 3′ UTRs and a poly(A) tail, as described previously.[18] The final mRNA utilized Cap1 to increase mRNA translation efficiency. After purification, the mRNA was diluted in citrate buffer to the desired concentration and frozen. Complete sequences and chemistry can be found in Tables S1 and S2.

LNP formulations were prepared by ethanol drop nanoprecipitation as described previously.[22] Briefly, heptadecan-9-yl 8-((2-hydroxyethyl)(8-(nonyloxy)-8-oxooctyl)amino)octanoate, dipalmitoylphosphatidylcholine, cholesterol, and 1,2-dimyristoyl-glycero-3-methoxypolyethylene glycol-2000 were dissolved in ethanol at molar ratios of 50:10:38.5:1.5, respectively, and combined with acidified mRNA (sodium acetate [pH 5]) at a ratio of 3:1 (aqueous:ethanol). Formulations were dialyzed against PBS (pH 7.4) in dialysis cassettes for at least

18 h. Formulations were concentrated using Amicon ultracentrifugal filters (EMD Millipore), passed through a 0.22-μm filter, and stored at 4°C until use. All formulations were tested for particle size, RNA encapsulation, and endotoxin and were found to be between 80–100 nm in size, with more than 80% encapsulation, and less than 10 endotoxin units (EU)/mL.

Animals

All mice used in this study were on the C57BL/6J genetic background. The development of *Ctrn*-KO mice and *mGPD*-KO mice has been described previously.[27,45] All WT, *Ctrn*-KO, *mGPD*-KO, and *Ctrn*/*mGPD*-dKO mice used in this study were generated based on the breeding strategy described previously by Saheki et al.[30] All animal studies were approved by the Ethical Committees for Animal Experimentation at Kagoshima University and The Institutional Animal Care and Use Committee at Moderna Therapeutics.

Oral Voluntary Sucrose Intake Test in Mice

Procedures for measuring voluntary oral sucrose intake in mice have been described previously.[28] Briefly, singly housed mice were simultaneously presented with bottles containing either pure water or 20% sucrose solution. In this study, the mice received three 0.5 mg/kg weekly i.v. injections of either a Ctrl mRNA (Ctrl) or hCitrin-mRNA$_{CoV}$ (hCitrin). Specifically, voluntary sucrose intake was assessed before and after administration of the second dose of mRNAs. The intake of pure water or sucrose solution was recorded for a total of 48 h either before or 24 h after i.v. administration of mRNAs (0.5 mg/kg). The position of the bottles was alternated every day to minimize conditioning. The preference index was recorded as the ratio of sucrose:water solution consumed as described previously described.[28]

Mammalian Cell Culture and Transfection

HeLa and HepG2 cells were obtained from the ATCC (Manassas, VA) and maintained under standard recommended conditions (Eagle's minimal essential medium [EMEM] supplied with 10% fetal bovine serum [FBS]). One day prior to transfection, 0.2–2.0 million cells were seeded into 6-well or 150-mm plates, resulting in approximately 70% confluency on the day of transfection. Cells were transfected with 1–20 μg of mRNA using Lipofectamine 2000 (Invitrogen) according to the manufacturer's instructions. Twenty-four hours post-transfection, cells were harvested and processed for whole-cell lysates or mitochondrial preparations.

Isolation of Mitochondria from Mammalian Cells or Livers

Isolation of mitochondrial fractions was performed using commercially available kits from Thermo Fisher Scientific (catalog number 89874). Briefly, liver sections or cultured cells were homogenized in mitochondrial isolation buffer (1:5, w/v) using a suitable glass Dounce homogenizer by stroking the samples 35 times on ice (first with loosely fitting pestle "A" 10 times, followed by tightly fitting pestle "B" 25 times). The homogenate was centrifuged at 1,000 × *g* for 10 min at 4°C. The resulting supernatant was transferred to a new vial and centrifuged at 12,000 × *g* for 10 min at 4°C. The resulting pellet was washed with mitochondrial isolation buffer by centrifugation at 7,000 × *g* for 10 min at 4°C. The final pellet was suspended in mitochondrial isolation buffer and represents the mitochondrial fraction. For the Mal/Asp shuttle activity assay, the mitochondrial preparations were used immediately after isolation. For protein the expression assay, the mitochondrial preparations were stored at −80°C for later use.

Protein Expression Analysis

Citrin protein expression levels in cell lysates or mitochondrial preps were determined by standard immunoblot analysis or by the Simple Western system (Sally Sue, Protein Simple, San Jose, CA). Total protein concentration in cell lysates and mitochondrial preparation samples was determined using the Pierce BCA Protein Assay Kit (Thermo Scientific). For immunoblot analysis, the lysates or mitochondrial preparation samples (containing 50–100 μg of total protein) were separated by 4%–12% SDS-PAGE and transferred to nitrocellulose membranes (iBlot2, Invitrogen) using standard procedures (method P0 as recommended by the manufacturer). The membranes were first incubated with Odyssey blocking buffer (part number 927-40000, LI-COR Biosciences, Lincoln, NE) for at least 1 h, followed by probing with the anti-citrin Abs NBP1-89019 (Novus) or TA-332958 (OriGene) or an anti-citrate synthase Ab, PA5-22126 (Thermo Fisher Scientific), for at least 1 h. Following incubation with the infrared (IR)-labeled goat anti-rabbit secondary Ab (IRDye 800CW, LI-COR Biosciences), IR intensity signals (corresponding to protein expression levels) were assessed using the imaging instrument Odyssey CLx (LI-COR Biosciences, Lincoln, NE). For the Simple Western system-based analysis, cell lysates were first separated by capillary electrophoresis based on the size of the proteins, and then proteins were probed with the primary citrin Ab NBP1-89019 and secondary Abs as recommended by the manufacturer (DM-001, Protein Simple, San Jose, CA), followed by fluorescence-based detection and quantification of the protein of interest.

Confocal Immunocytochemistry Analysis

Hep3b (ATTC) cells were plated in 96-well, plastic-bottom plates (6055302, Perkin Elmer), using recommended culturing conditions, at a density of 15,000 cells per well. Cells were either kept non-transfected or transfected with the hCitrin-mRNA$_{WT}$ using Lipofectamine 2000. 24 h post-transfection, the cells were fixed in 4% paraformaldehyde (PFA) and processed for immunofluorescent staining with anti-Citrin rabbit Ab (NBP1-89019, Novus) and anti-TOM20 mouse Ab (612278, BD Biosciences) to examine mitochondrial localization. Secondary Ab incubation was used to amplify the signal (goat anti-rabbit Alexa 488 and goat anti-mouse Alexa 647, respectively). The cells were counterstained with DAPI for nucleus visualization. Additional samples were stained only with the mitochondrial marker anti-TOM20 as a negative colocalization control. For image acquisition and colocalization analysis, samples were imaged on the Opera Phenix spinning disk confocal microscope (Perkin Elmer) using a 63× water immersion objective (NA 1.15). 16 fields of view (~40 cells each) were imaged for each sample. The TOM20 mitochondrial marker was imaged with the 647-nm laser line, the hCitrin was

imaged with the 488-nm laser line, and the nuclear stain was imaged with the 405-nm laser line. A z stack of five optical sections spanning 2 μm was acquired for all three channels. Images analysis was performed in Harmony, using a custom script to calculate the Pearson's co-localization coefficient (values above zero denote statistical significant co-localization between the channels of interest).

Mal/Asp Shuttle Activity Assay

The Mal/Asp activities were measured as described previously by Scholz and Koppenhafer,[46] with some modifications. Briefly, in a 96-well plate, 10–20 μL of mitochondria (20–30 mg/mL) were mixed with 130–140 μL of an assay buffer (300 mM mannitol, 10 mM potassium phosphate, 10 mM Tris, 10 mM KCl, and 5 mM magnesium chloride [pH 7.4]) supplemented with 2 mM Asp, 2 mM ADP, 4 mM Mal, 4 mM glutamate, 140 μM NADH, 5 U/mL of Mal dehydrogenase (MDH), and 5 U/mL of Asp transaminase (AST). The oxidation of NADH was monitored at 340 nm over time at 37°C using a BioTek Instruments plate reader (Synergy H1 hybrid reader) operated with the Gen5 software. The specific Mal/Asp shuttle activity was normalized to the rate of NADH oxidation in the absence of substrates (Mal and glutamate).

LC-MS Analysis of Citrulline

The levels of citrulline in liver homogenates and plasma were determined by liquid chromatography-mass spectrometry (LC-MS) with an Agilent 1290 Infinity LC system and an Agilent Technologies 6460 triple quadrupole MS detector. Liver homogenates were prepared by homogenizing liver tissues (~0.4 g) in 10 volumes (~4 mL) of distilled water (dH_2O) with a Dounce homogenizer (20 strokes), followed by a quick centrifugation (1,000 × *g* for 10 min) to remove nuclei. For protein precipitation, an aliquot of nucleus-depleted liver homogenates or plasma was mixed with 3 volumes of acetonitrile and centrifuged at 10,000 × *g* for 20 min. Ten μl of the deproteinized supernatant was separated by the InfinityLab Poroshell 120 hydrophilic interaction liquid chromatography (HILIC) 1.9 μm column (2.1 × 150 mm). The high-performance liquid chromatography (HPLC) mobile phases were 10 mM ammonium formate in dH_2O (pH 3) (A) and acetonitrile containing 10% of A (B). The flow rate was 0.4 mL/min, and the column temperature was kept at 30°C. The amount of A in the mobile phase was increased linearly from 5% to 70% over 5 min, followed by a rapid decrease to the initial condition (5% of A) in 0.1 min, and kept running for another 4.9 min before injection of the next sample. Citrulline (*m/z* 176.2) was detected in the MS detector operated in the positive mode.

Plasma Ammonia Analysis

Plasma ammonia was detected using a commercially available kit (Abnova, Walnut, CA; catalog number KA3707). In this assay, ammonia is used to form indophenol, a product that is easily detected by colorimetry (optical density 670 [OD_{670}]), and the amount of ammonium in a testing samples is determined by a standard curve generated by a series of ammonium chloride ranging from 2 to 100 μM.

Statistical Analysis

Data are expressed as means ± SEM. Means were compared by unpaired (two groups) or paired t test (to compare pre- and post-treatment values) and one-way or two-way ANOVA. Significant ANOVA findings were followed by Tukey's *post hoc* test for multiple comparisons. All statistical analyses were performed using Prism 7 (GraphPad) software. A p value of less than 0.05 was considered statistically significant.

Data Availability

The datasets generated and/or analyzed during the current study are available from the corresponding author upon request.

SUPPLEMENTAL INFORMATION

Supplemental Information can be found online at https://doi.org/10.1016/j.ymthe.2019.04.017.

AUTHOR CONTRIBUTIONS

Conceptualization, P.M.; Methodology, J.C., D.A., J. Santana, C.M., G.B., C.L., L.G., P.F., P.H.G., T. Salerno, and P.M.; Data Acquisition, Curation, and Analysis, J.C., D.A., M.G., J.Z., S.L., M.E., A. Frassetto, E.K., A. Funahashi, J. Santana, C.M., K.E.B., E.S.K., S.S., T. Salerno, T.F., K.C., B.L., J. Schultz, and T. Saheki; Writing – Original Draft, J.C. and T. Saheki; Writing – Review and Editing, J.C., E.J.M., P.H.G., and P.M.; Supervision, P.H.G. and P.M.

CONFLICTS OF INTERESTS

J.C., J.A., J.Z., S.L., M.E., A. Frassetto, J. Santana, C.M., K.E.B., E.S.K., S.S., T. Salerno, K.C., E.J.M., B.L., G.B., J. Schultz, C.L., L.G., P.F., P.H.G., and P.M. are employees of and received salary and stock options from Moderna, Inc. (Cambridge, MA, USA).

ACKNOWLEDGMENTS

The authors thank Dr. Serenus Hua, Srujan Gandham, and Penggao Duan (Department of Chemistry, Moderna, Cambridge, MA, USA) for support with LC-MS assay development. We thank Vlad Presnyak (Bioinformatics and Computational Science, Moderna, Cambridge, MA, USA) for support with codon-optimization design. We thank colleagues from Moderna's production teams for sourcing mRNA constructs and formulations. We also thank Dr. David Sinasac from the Biochemical Genetics Laboratory, Alberta Children's Hospital for helpful discussions related to biochemical assays and mouse models. Finally, we thank our colleagues Izumi Yasuda, Yoshiko Setogawa, and Toru Obara for constructive discussions regarding the manuscript.

REFERENCES

1. Kobayashi, K., Sinasac, D.S., Iijima, M., Boright, A.P., Begum, L., Lee, J.R., Yasuda, T., Ikeda, S., Hirano, R., Terazono, H., et al. (1999). The gene mutated in adult-onset type II citrullinaemia encodes a putative mitochondrial carrier protein. Nat. Genet. *22*, 159–163.

2. Palmieri, L., Pardo, B., Lasorsa, F.M., del Arco, A., Kobayashi, K., Iijima, M., Runswick, M.J., Walker, J.E., Saheki, T., Satrústegui, J., and Palmieri, F. (2001). Citrin and aralar1 are Ca(2+)-stimulated aspartate/glutamate transporters in mitochondria. EMBO J. *20*, 5060–5069.

3. Saheki, T., and Kobayashi, K. (2002). Mitochondrial aspartate glutamate carrier (citrin) deficiency as the cause of adult-onset type II citrullinemia (CTLN2) and idiopathic neonatal hepatitis (NICCD). J. Hum. Genet. *47*, 333–341.

4. Meijer, A.J., Gimpel, J.A., Deleeuw, G., Tischler, M.E., Tager, J.M., and Williamson, J.R. (1978). Interrelationships between gluconeogenesis and ureogenesis in isolated hepatocytes. J. Biol. Chem. *253*, 2308–2320.

5. Saheki, T., Ueda, A., Hosoya, M., Kusumi, K., Takada, S., Tsuda, M., and Katsunuma, T. (1981). Qualitative and quantitative abnormalities of argininosuccinate synthetase in citrullinemia. Clin. Chim. Acta *109*, 325–335.

6. Saheki, T., Ueda, A., Iizima, K., Yamada, N., Kobayashi, K., Takahashi, K., and Katsunuma, T. (1982). Argininosuccinate synthetase activity in cultured skin fibroblasts of citrullinemic patients. Clin. Chim. Acta *118*, 93–97.

7. Saheki, T., Kobayashi, K., Iijima, M., Nishi, I., Yasuda, T., Yamaguchi, N., Gao, H.Z., Jalil, M.A., Begum, L., and Li, M.X. (2002). Pathogenesis and pathophysiology of citrin (a mitochondrial aspartate glutamate carrier) deficiency. Metab. Brain Dis. *17*, 335–346.

8. Song, Y.Z., Deng, M., Chen, F.P., Wen, F., Guo, L., Cao, S.L., Gong, J., Xu, H., Jiang, G.Y., Zhong, L., et al. (2011). Genotypic and phenotypic features of citrin deficiency: five-year experience in a Chinese pediatric center. Int. J. Mol. Med. *28*, 33–40.

9. Tazawa, Y., Kobayashi, K., Ohura, T., Abukawa, D., Nishinomiya, F., Hosoda, Y., Yamashita, M., Nagata, I., Kono, Y., Yasuda, T., et al. (2001). Infantile cholestatic jaundice associated with adult-onset type II citrullinemia. J. Pediatr. *138*, 735–740.

10. Tomomasa, T., Kobayashi, K., Kaneko, H., Shimura, H., Fukusato, T., Tabata, M., Inoue, Y., Ohwada, S., Kasahara, M., Morishita, Y., et al. (2001). Possible clinical and histologic manifestations of adult-onset type II citrullinemia in early infancy. J. Pediatr. *138*, 741–743.

11. Hayasaka, K., Numakura, C., Toyota, K., Kakizaki, S., Watanabe, H., Haga, H., Takahashi, H., Takahashi, Y., Kaneko, M., Yamakawa, M., et al. (2014). Medium-chain triglyceride supplementation under a low-carbohydrate formula is a promising therapy for adult-onset type II citrullinemia. Mol. Genet. Metab. Rep. *1*, 42–50.

12. Hayasaka, K., Numakura, C., Toyota, K., and Kimura, T. (2012). Treatment with lactose (galactose)-restricted and medium-chain triglyceride-supplemented formula for neonatal intrahepatic cholestasis caused by citrin deficiency. JIMD Rep. *2*, 37–44.

13. Kimura, N., Kubo, N., Narumi, S., Toyoki, Y., Ishido, K., Kudo, D., Umehara, M., Yakoshi, Y., and Hakamada, K. (2013). Liver transplantation versus conservative treatment for adult-onset type II citrullinemia: our experience and a review of the literature. Transplant. Proc. *45*, 3432–3437.

14. Kogure, T., Kondo, Y., Kakazu, E., Ninomiya, M., Kimura, O., Kobayashi, N., and Shimosegawa, T. (2014). Three cases of adult-onset type II citrullinemia treated with different therapies: Efficacy of sodium pyruvate and low-carbohydrate diet. Hepatol. Res. *44*, 707–712.

15. Parenti, G., Andria, G., and Ballabio, A. (2015). Lysosomal storage diseases: from pathophysiology to therapy. Annu. Rev. Med. *66*, 471–486.

16. Donsante, A., Miller, D.G., Li, Y., Vogler, C., Brunt, E.M., Russell, D.W., and Sands, M.S. (2007). AAV vector integration sites in mouse hepatocellular carcinoma. Science *317*, 477.

17. An, D., Schneller, J.L., Frassetto, A., Liang, S., Zhu, X., Park, J.S., Theisen, M., Hong, S.J., Zhou, J., Rajendran, R., et al. (2017). Systemic Messenger RNA Therapy as a Treatment for Methylmalonic Acidemia. Cell Rep. *21*, 3548–3558.

18. Richner, J.M., Himansu, S., Dowd, K.A., Butler, S.L., Salazar, V., Fox, J.M., Julander, J.G., Tang, W.W., Shresta, S., Pierson, T.C., et al. (2017). Modified mRNA Vaccines Protect against Zika Virus Infection. Cell *169*, 176.

19. Bahl, K., Senn, J.J., Yuzhakov, O., Bulychev, A., Brito, L.A., Hassett, K.J., Laska, M.E., Smith, M., Almarsson, Ö., Thompson, J., et al. (2017). Preclinical and Clinical Demonstration of Immunogenicity by mRNA Vaccines against H10N8 and H7N9 Influenza Viruses. Mol. Ther. *25*, 1316–1327.

20. Hewitt, S.L., Bai, A., Bailey, D., Ichikawa, K., Zielinski, J., Karp, R., Apte, A., Arnold, K., Zacharek, S.J., Iliou, M.S., et al. (2019). Durable anticancer immunity from intratumoral administration of IL-23, IL-36γ, and OX40L mRNAs. Sci. Transl. Med. *11*, eaat9143.

21. Jiang, L., Berraondo, P., Jericó, D., Guey, L.T., Sampedro, A., Frassetto, A., Benenato, K.E., Burke, K., Santamaría, E., Alegre, M., et al. (2018). Systemic messenger RNA as an etiological treatment for acute intermittent porphyria. Nat. Med. *24*, 1899–1909.

22. Sabnis, S., Kumarasinghe, E.S., Salerno, T., Mihai, C., Ketova, T., Senn, J.J., Lynn, A., Bulychev, A., McFadyen, I., Chan, J., et al. (2018). A Novel Amino Lipid Series for mRNA Delivery: Improved Endosomal Escape and Sustained Pharmacology and Safety in Non-human Primates. Mol. Ther. *26*, 1509–1519.

23. Iwahashi, J., Yamazaki, S., Komiya, T., Nomura, N., Nishikawa, S., Endo, T., and Mihara, K. (1997). Analysis of the functional domain of the rat liver mitochondrial import receptor Tom20. J. Biol. Chem. *272*, 18467–18472.

24. Cullis, P.R., and Hope, M.J. (2017). Lipid Nanoparticle Systems for Enabling Gene Therapies. Mol. Ther. *25*, 1467–1475.

25. Ball, R.L., Hajj, K.A., Vizelman, J., Bajaj, P., and Whitehead, K.A. (2018). Lipid Nanoparticle Formulations for Enhanced Co-delivery of siRNA and mRNA. Nano Lett. *18*, 3814–3822.

26. Mauro, V.P., and Chappell, S.A. (2014). A critical analysis of codon optimization in human therapeutics. Trends Mol. Med. *20*, 604–613.

27. Sinasac, D.S., Moriyama, M., Jalil, M.A., Begum, L., Li, M.X., Iijima, M., Horiuchi, M., Robinson, B.H., Kobayashi, K., Saheki, T., and Tsui, L.C. (2004). Slc25a13-knockout mice harbor metabolic deficits but fail to display hallmarks of adult-onset type II citrullinemia. Mol. Cell. Biol. *24*, 527–536.

28. Saheki, T., Inoue, K., Ono, H., Fujimoto, Y., Furuie, S., Yamamura, K.I., Kuroda, E., Ushikai, M., Asakawa, A., Inui, A., et al. (2017). Oral aversion to dietary sugar, ethanol and glycerol correlates with alterations in specific hepatic metabolites in a mouse model of human citrin deficiency. Mol. Genet. Metab. *120*, 306–316.

29. Nakamura, M., Yazaki, M., Kobayashi, Y., Fukushima, K., Ikeda, S., Kobayashi, K., Saheki, T., and Nakaya, Y. (2011). The characteristics of food intake in patients with type II citrullinemia. J. Nutr. Sci. Vitaminol. (Tokyo) *57*, 239–245.

30. Saheki, T., Iijima, M., Li, M.X., Kobayashi, K., Horiuchi, M., Ushikai, M., Okumura, F., Meng, X.J., Inoue, I., Tajima, A., et al. (2007). Citrin/mitochondrial glycerol-3-phosphate dehydrogenase double knock-out mice recapitulate features of human citrin deficiency. J. Biol. Chem. *282*, 25041–25052.

31. Takahashi, H., Kagawa, T., Kobayashi, K., Hirabayashi, H., Yui, M., Begum, L., Mine, T., Takagi, S., Saheki, T., and Shinohara, Y. (2006). A case of adult-onset type II citrullinemia–deterioration of clinical course after infusion of hyperosmotic and high sugar solutions. Med. Sci. Monit. *12*, CS13–CS15.

32. Chong, S.C., Lo, P., Chow, C.W., Yuen, L., Chu, W.C.W., Leung, T.Y., Hui, J., and Scaglia, F. (2018). Molecular and clinical characterization of citrin deficiency in a cohort of Chinese patients in Hong Kong. Mol. Genet. Metab. Rep. *17*, 3–8.

33. Saheki, T., Inoue, K., Tushima, A., Mutoh, K., and Kobayashi, K. (2010). Citrin deficiency and current treatment concepts. Mol. Genet. Metab. *100* (*Suppl 1*), S59–S64.

34. Saheki, T., and Song, Y.Z. (1993). Citrin deficiency. In GeneReviews, M.P. Adam, H.H. Ardinger, and R.A. Pagon, et al., eds. (Seattle, WA: University of Seattle), https://www.ncbi.nlm.nih.gov/books/NBK1181.

35. Zhao, X.B., and Lee, R.J. (2004). Tumor-selective targeted delivery of genes and antisense oligodeoxyribonucleotides via the folate receptor. Adv. Drug Deliv. Rev. *56*, 1193–1204.

36. Akinc, A., Querbes, W., De, S., Qin, J., Frank-Kamenetsky, M., Jayaprakash, K.N., Jayaraman, M., Rajeev, K.G., Cantley, W.L., Dorkin, J.R., et al. (2010). Targeted delivery of RNAi therapeutics with endogenous and exogenous ligand-based mechanisms. Mol. Ther. *18*, 1357–1364.

37. DeRosa, F., Guild, B., Karve, S., Smith, L., Love, K., Dorkin, J.R., Kauffman, K.J., Zhang, J., Yahalom, B., Anderson, D.G., and Heartlein, M.W. (2016). Therapeutic efficacy in a hemophilia B model using a biosynthetic mRNA liver depot system. Gene Ther. *23*, 699–707.

38. Fenton, O.S., Kauffman, K.J., McClellan, R.L., Appel, E.A., Dorkin, J.R., Tibbitt, M.W., Heartlein, M.W., DeRosa, F., Langer, R., and Anderson, D.G. (2016). Bioinspired Alkenyl Amino Alcohol Ionizable Lipid Materials for Highly Potent In Vivo mRNA Delivery. Adv. Mater. *28*, 2939–2943.

39. Kauffman, K.J., Mir, F.F., Jhunjhunwala, S., Kaczmarek, J.C., Hurtado, J.E., Yang, J.H., Webber, M.J., Kowalski, P.S., Heartlein, M.W., DeRosa, F., and Anderson, D.G. (2016). Efficacy and immunogenicity of unmodified and pseudouridine-modified

mRNA delivered systemically with lipid nanoparticles in vivo. Biomaterials *109*, 78–87.

40. Tazawa, Y., Kobayashi, K., Abukawa, D., Nagata, I., Maisawa, S., Sumazaki, R., Iizuka, T., Hosoda, Y., Okamoto, M., Murakami, J., et al. (2004). Clinical heterogeneity of neonatal intrahepatic cholestasis caused by citrin deficiency: case reports from 16 patients. Mol. Genet. Metab. *83*, 213–219.

41. Yasuda, T., Yamaguchi, N., Kobayashi, K., Nishi, I., Horinouchi, H., Jalil, M.A., Li, M.X., Ushikai, M., Iijima, M., Kondo, I., and Saheki, T. (2000). Identification of two novel mutations in the SLC25A13 gene and detection of seven mutations in 102 patients with adult-onset type II citrullinemia. Hum. Genet. *107*, 537–545.

42. Kikuchi, A., Arai-Ichinoi, N., Sakamoto, O., Matsubara, Y., Saheki, T., Kobayashi, K., Ohura, T., and Kure, S. (2012). Simple and rapid genetic testing for citrin deficiency by screening 11 prevalent mutations in SLC25A13. Mol. Genet. Metab. *105*, 553–558.

43. Kobayashi, K., Bang Lu, Y., Xian Li, M., Nishi, I., Hsiao, K.J., Choeh, K., Yang, Y., Hwu, W.L., Reichardt, J.K., Palmieri, F., et al. (2003). Screening of nine SLC25A13 mutations: their frequency in patients with citrin deficiency and high carrier rates in Asian populations. Mol. Genet. Metab. *80*, 356–359.

44. Lin, W.X., Zeng, H.S., Zhang, Z.H., Mao, M., Zheng, Q.Q., Zhao, S.T., Cheng, Y., Chen, F.P., Wen, W.R., and Song, Y.Z. (2016). Molecular diagnosis of pediatric patients with citrin deficiency in China: SLC25A13 mutation spectrum and the geographic distribution. Sci. Rep. *6*, 29732.

45. Eto, K., Tsubamoto, Y., Terauchi, Y., Sugiyama, T., Kishimoto, T., Takahashi, N., Yamauchi, N., Kubota, N., Murayama, S., Aizawa, T., et al. (1999). Role of NADH shuttle system in glucose-induced activation of mitochondrial metabolism and insulin secretion. Science *283*, 981–985.

46. Scholz, T.D., and Koppenhafer, S.L. (1995). Reducing equivalent shuttles in developing porcine myocardium: enhanced capacity in the newborn heart. Pediatr. Res. *38*, 221–227.

YMTHE, Volume *27*

Supplemental Information

mRNA Therapy Improves Metabolic and Behavioral Abnormalities in a Murine Model of Citrin Deficiency

Jingsong Cao, Ding An, Mikel Galduroz, Jenny Zhuo, Shi Liang, Marianne Eybye, Andrea Frassetto, Eishi Kuroda, Aki Funahashi, Jordan Santana, Cosmin Mihai, Kerry E. Benenato, E. Sathyajith Kumarasinghe, Staci Sabnis, Timothy Salerno, Kimberly Coughlan, Edward J. Miracco, Becca Levy, Gilles Besin, Joshua Schultz, Christine Lukacs, Lin Guey, Patrick Finn, Tatsuhiko Furukawa, Paloma H. Giangrande, Takeyori Saheki, and Paolo G.V. Martini

SUPPLEMENTARY FIGURES

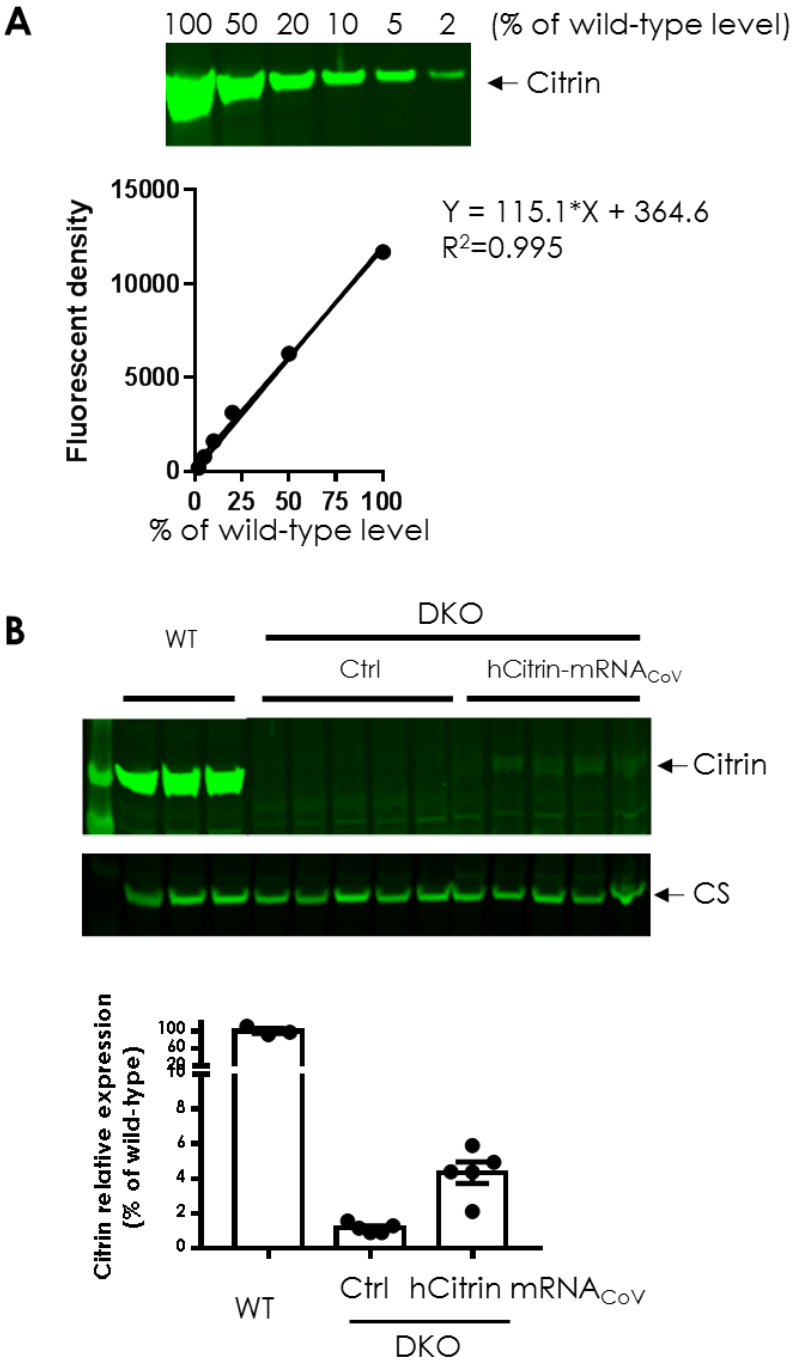

Supplementary Fig. 1. hCitrin protein levels in citrin deficient mice (*Ctrn*$^{-/-}$). A) Immunoblot of increasing amounts of citrin protein from wild-type mouse liver mitochondrial extracts for generating citrin protein standard curve. The quantitative fluorescent signals from the citrin bands were plotted against the percentage of citrin protein expression level in wild-type mice,

showing a wide range of linearity. **B)** Citrin protein expression levels in citrin deficient mice (*Ctrn*$^{-/-}$) after repeat injections of hCitrn-mRNA. *Ctrn/mGPD*-dKO mice received three weekly injections (*i.v.*) of either control (Ctrl) or hCitrin-mRNA$_{CoV}$ at 0.5 mg/kg. Mice were euthanized at 24 hr after the third and final injection. Citrin protein expression levels in mitochondria prepared from mouse livers were assessed by Western blot analysis, normalized to Citrate Synthase (CS), a mitochondrial marker, and expressed as percentage of the average of wild-type group. The average hCitrin protein expression level introduced to the *Ctrn/mGPD*-dKO was 4.3% of wild-type level in mice. Citrin and CS protein expression levels were quantified using the Odyssey CLx instrument and accompanying software. WT, wild-type mice. Bars represent mean ± SEM (n = 3 – 5).

SUPPLEMENTARY TABLES

Supplementary Table 1. Complete mRNA sequence of hCitrin-mRNA$_{CoV}$. U = 5-methoxyuridine. UTR sequences are underlined.

GGGAAAUAAGAGAGAAAAGAAGAGUAAGAAGAAAUAUAAGAGCCACCAUGGCCGCCGCCAAGGU
CGCCCUCACCAAGAGGGCGGACCCCGCGGAGCUCAGGACCAUCUUUCUCAAGUACGCCUCCAUCG
AGAAGAACGGGGAGUUCUUCAUGAGCCCGAACGAUUUCGUCACCAGGUACCUCAACAUCUUCGG
CGAGAGCCAGCCCAACCCGAAGACCGUAGAGCUCCUCAGCGGCGUCGUCGACCAGACGAAGGACG
GACUCAUUAGCUUCCAGGAGUUCGUCGCCUUCGAGAGCGUCCUCUGCGCGCCCGACGCCCUCUU
CAUGGUCGCGUUCCAGCUGUUCGAUAAGGCCGGCAAGGGCGAGGUGACCUUUGAAGAUGUGAA
GCAGGUGUUCGGUCAGACCACCAUCCACCAGCACAUCCCUUUUAACUGGGACUCAGAAUUCGUC
CAGCUGCACUUCGGCAAGGAAAGGAAGCGCCAUCUGACCUACGCCGAGUUCACACAGUUUCUCC
UGGAGAUCCAGCUGGAACACGCCAAACAGGCGUUCGUUCAGCGGGACAACGCCAGGACCGGCCG
GGUCACCGCGAUCGACUUCCGUGAUAUCAUGGUGACCAUCAGGCCUCACGUCCUGACGCCCUUC
GUGGAAGAGUGCCUGGUGGCCGCCGCGGGUGGGACCACGUCCCACCAGGUGAGCUUCUCCUAU
UUUAACGGGUUCAACAGCCUCCUCAACAACAUGGAGCUGAUCCGGAAGAUCUAUAGCACCCUGG
CCGGGACGCGCAAGGACGUCGAGGUGACCAAGGAAGAAUUCGUGCUGGCCGCCCAGAAGUUUG
GCCAGGUGACGCCCAUGGAGGUGGACAUCCUGUUCCAACUGGCGGACCUGUACGAACCCAGGGG
CCGGAUGACCCUGGCCGACAUCGAGCGCAUUGCCCCGCUCGAGGAGGGCACCCUGCCCUUCAACC
UGGCGGAGGCCCAGCGCCAGAAGGCCAGCGGGGACAGCGCCAGGCCCGUCCUGCUGCAGGUGGC
CGAGUCCGCGUACAGGUUCGGUCUGGGGAGCGUCGCGGGAGCCGUGGGUGCCACCGCCGUGUA
UCCGAUCGACCUCGUGAAGACCCGUAUGCAGAAUCAGAGGUCCACCGGCAGCUUCGUGGGCGAG
CUCAUGUACAAGAACUCCUUCGACUGUUUCAAGAAGGUUCUCCGGUACGAGGGGUUCUUCGGC
CUCUACCGGGGACUGCUACCCCAGCUGCUCGGCGUGGCGCCCGAGAAGGCCAUCAAGCUCACGG
UCAACGACUUUGUGCGGGACAAGUUCAUGCACAAGGACGGCAGCGUCCCACUGGCCGCCGAGAU
UCUGGCAGGCGGCUGCGCCGGAGGCAGCCAGGUCAUCUUUACCAACCCACUGGAGAUCGUGAAG
AUCAGGCUGCAAGUGGCCGGGGAGAUUACCACCGGACCCCGUGUGAGCGCCCUGAGCGUGGUG
AGGGACCUUGGCUUCUUUGGCAUAUACAAGGGAGCCAAGGCCUGCUUUCUGAGGGACAUCCCG
UUUUCCGCCAUAUACUUUCCCUGCUACGCCCACGUGAAAGCGAGCUUCGCCAACGAGGACGGCC
AGGUCAGUCCCGGCUCCCUACUGCUGGCCGGAGCCAUCGCCGGGAUGCCCGCCGCCAGCCUGGU
GACGCCCGCGGACGUUAUCAAGACCAGGCUGCAGGUGGCGGCCAGGGCGGGCCAGACCACCUAC
AGCGGCGUGAUCGACUGCUUCCGCAAGAUCCUGCGGGAGGAGGGGCCCAAGGCCCUGUGGAAA
GGCGCCGGGGCAAGGGUGUUCAGGAGCAGCCCACAGUUCGGGGUGACCCUGCUUACCUACGAAC
UGCUGCAGCGGUGGUUCUAUAUCGACUUCGGAGGAGUCAAGCCCAUGGGCUCCGAGCCUGUGC
CCAAGAGCAGGAUCAAUCUGCCCGCGCCCAACCCAGACCACGUGGGAGGGUACAAACUGGCCGUG
GCCACCUUCGCCGGAAUCGAGAACAAGUUCGGCCUGUAUCUGCCCCUGUUCAAACCGUCCGUCU
CCACCAGCAAGGCCAUCGGCGGAGGCCCCUGAUAAUAGUCCAUAAAGUAGGAAACACUACAGCU
GGAGCCUCGGUGGCCAUGCUUCUUGCCCCUUGGGCCUCCCCCCAGCCCCUCCUCCCCUUCCUGCA
CCCGUACCCCCCGCAUUAUUACUCACGGUACGAGUGGUCUUUGAAUAAAGUCUGAGUGGGCGG
CAAAAAAAAAAAAAAAAAAAAAAAAAAAAAAAAAAAAAAAAAAAAAAAAAAAAAAAAAAAAAA
AAAAAAAAAAAAAAAAAAAAAAAAAAAAAAAAAAAUCUAG

Supplementary Table 2. Complete mRNA sequence of eGFP. U = N1m-pseudouridine. UTR sequences are underlined.

GGGAAAUAAGAGAGAAAAGAAGAGUAAGAAGAAAUAUAAGAGCCACCAUGGUGUCCAAGGGUG
AGGAAUUGUUUACCGGGGUGGUGCCUAUUCUCGUCGAACUUGACGGGGAUGUGAAUGGACAC
AAGUUUUCGGUAUCCGGAGAAGGAGAGGGUGACGCCACAUACGGAAAGCUUACACUCAAAUUC
AUCUGUACGACGGGGAAACUGCCCGUACCCUGGCCUACGCUCGUAACCACGCUGACUUAUGGAG
UGCAGUGCUUUAGCAGAUACCCCGACCAUAUGAAGCAGCACGACUUCUUCAAGUCGGCGAUGCC
CGAGGGGUACGUGCAAGAGAGGACCAUUUUCUUCAAAGACGAUGGCAAUUACAAAACACGCGCA
GAAGUCAAGUUUGAGGGCGAUACUCUGGUCAAUCGGAUCGAAUUGAAGGGAAUCGAUUUCAAA
GAAGAUGGAAACAUCCUUGGCCAUAAGCUCGAGUACAACUAUAACUCGCAUAAUGUCUAUAUCA
UGGCUGACAAGCAGAAAAACGGUAUCAAAGUCAACUUUAAGAUCCGACACAAUAUUGAGGACGG
UUCGGUGCAGCUUGCGGACCACUAUCAACAGAAUACGCCGAUUGGGGAUGGUCCGGUCCUUUU
GCCGGAUAACCAUUAUCUCUCAACCCAGUCAGCCCUGAGCAAAGAUCCAAACGAGAAGAGGGACC
ACAUGGUCUUGCUCGAAUUCGUGACAGCGGCAGGGAUCACUCUGGGAAUGGACGAGUUGUACA
AGUGAUAAUAGGCUGGAGCCUCGGUGGCCAUGCUUCUUGCCCCUUGGGCCUCCCCCCAGCCCCU
CCUCCCCUUCCUGCACCCGUACCCCCGUGGUCUUUGAAUAAAGUCUGAGUGGGCGGCAAAAAAA
AAAAAAAAAAAAAAAAAAAAAAAAAAAAAAAAAAAAAAAAAAAAAAAAAAAAAAAAAAAAAAAA
AAAAAAAAAAAAAAAAAAAAAAAAAAAUCUAG